Consistency Analysis of EKF-based SLAM by Measurement Noise and Observation Times

LI Hui-Ping[1] XU De-Min[1] ZHANG Fu-Bin[1] YAO Yao[1]

Abstract Inconsistency is a fundamental problem in simultaneous localization and mapping (SLAM). Previous works from predecessors have studied the inconsistent problem of extended Kalman filter (EKF) SLAM algorithm focusing on the linearization errors. In this paper, we studied the inconsistency issue of EKF SLAM in theory based on measurement noise and observation time. In a simplified situation, we deduced some useful theorems of estimated covariance matrix. Then, we made use of them to investigate the inconsistency issue. We showed that the measurement noise and the observation times can drive the EKF SLAM out of consistency. Moreover, we demonstrated the explicit effects of measurement noise and observation times on inconsistency of the EKF SLAM. Our simulation experiments verified the results.

Key words Simultaneous localization and mapping (SLAM), extended Kalman filter (EKF), consistency, measurement noise, observation times

Simultaneous localization and mapping (SLAM) is the process of the robot building a map of an environment, while concurrently localizing itself in it. A solution to the SLAM problem has been seen as a "holy grail" for the mobile robotics community as it would provide a means to make a robot truly autonomous. The stochastic solution to SLAM was proposed by Smith[1], which was the first to formally address measurement error correlations that arise during the map-building process. Many different solutions[1−7] to SLAM have been proposed during the past 20 years, for SLAM algorithm is the main solution to SLAM problem[8−9], for EKF SLAM has been formulated and solved as a theoretical problem in a number of different forms. To implement the EKF SLAM in practice, many variants[2−5, 7] were put forward to reduce computational complexity, and others[10−12] dealt with data association. However, in spite of its clear success in practical applications, the fundamental consistency of the SLAM algorithm has received little attention. Earlier works[13−20] on EKF-SLAM consistency showed that eventual inconsistency of the algorithm is inevitable for large-scale maps, and the estimated uncertainty will become optimistic when compared to the true errors. Julier[15] took a counter example to show the inconsistency issue in EKF SLAM. Then, some papers[13, 19−20] showed that the inconsistent estimate is because of the errors introduced by the linearization process and can be inevitable. Bailey[16] used Monte Carlo simulations to investigate whether the degree of inconsistency was always significant and under what conditions EKF-SLAM might produce reasonable results. Huang[14] has provided a theoretical explanation to inconsistency and gained some theoretical results: the violation of some fundamental constraints governing the relationship between various Jacobians, when they are evaluated at the current state estimate may cause inconsistency. Based on the analysis on inconsistency, some algorithms[18, 21−22] have been proposed to improve the consistency of EKF SLAM. However, no previous work has investigated whether the measurement noise could cause the inconsistency, what is the effect on inconsistency and why it is inevitable when observation time increases. In this paper, we will provide explicit formula for the covariance matrices for a basic scenario in the nonlinear two-dimensional EKF SLAM problem with point landmarks observed using a range-and-bearing sensor. Theoretical proofs of measurement noise effect and observation time effect on inconsistency are given. Through explicit analysis, our results are: 1) The measurement noise is a factor to cause EKF SLAM inconsistency; with increase in the value of measurement noise, the degree of inconsistency will decrease; with the observation times increase, the algorithm will inevitably become inconsistent, but the inconsistency caused by it will reach an upper bound; 2) The degree of improvement to consistency by increasing the measurement noise is greater than the degree of damage to consistency by increasing the observation time.

Received June 26, 2008; in revised form December 20, 2008
Supported by the Doctorate Foundation of Northwestern Polytechnical University (CX200701)
1. College of Marine Engineering, Northwestern Polytechnical University, Xi′an 710072, P. R. China
DOI: 10.3724/SP.J.1004.2009.01177

1 EKF SLAM algorithm

In this section, to make use of some results in [14], we use the same robot model suitable for theoretical analysis. We specify the SLAM state as the robot pose (heading and position) and localization of stationary landmarks observed in the environment. The state at time k is represented by a joint state-vector $\boldsymbol{X}(k)$ as

$$\boldsymbol{X}(k) = \begin{bmatrix} \phi(k) \\ \boldsymbol{X}_r(k) \\ \boldsymbol{m} \end{bmatrix} \tag{1}$$

where $\phi(k)$ is the robot heading orientation, $\boldsymbol{X}_r(k) = \begin{bmatrix} x_r(k) & y_r(k) \end{bmatrix}^{\mathrm{T}}$ is the robot position, and $\boldsymbol{m} = \begin{bmatrix} \boldsymbol{X}_1(k) & \boldsymbol{X}_2(k) & \cdots & \boldsymbol{X}_N(k) \end{bmatrix}^{\mathrm{T}}$ is the positions of landmarks.

1.1 Process model and observation model

To describe the robot motion, we use the kinematical model for the trajectory of the front wheel of a bicycle subjected to rolling motion constraints (i.e., assuming zero wheel slip). The robot is shown in Fig. 1. The discrete form of robot model is represented by

$$\begin{bmatrix} \phi(k+1) \\ \boldsymbol{X}_r(k+1) \end{bmatrix} = \boldsymbol{f}(\phi(k), \boldsymbol{X}_r(k), \boldsymbol{u}_r(k)) \tag{2}$$

$$\boldsymbol{f}(\phi(k), \boldsymbol{X}_r(k), \boldsymbol{u}_r(k)) = \begin{bmatrix} \phi(k) + \dfrac{(\nu(k)+\delta\nu)T\sin(\gamma(k)+\delta\gamma)}{L} \\ x_r(k) + (\nu(k)+\delta\nu)T\cos(\phi(k)) \\ y_r(k) + (\nu(k)+\delta\nu)T\cos(\phi(k)) \end{bmatrix} \tag{3}$$

where $\boldsymbol{u} = \begin{bmatrix} \nu(k) & \gamma(k) \end{bmatrix}^{\mathrm{T}}$ are termed control inputs. L is the wheelbase between the front and rear axles. $\delta\nu$ and

$\delta\gamma$ are zero-mean Gaussian white noises on $\nu(k)$ and $\gamma(k)$, respectively. T is the time interval between the two steps.

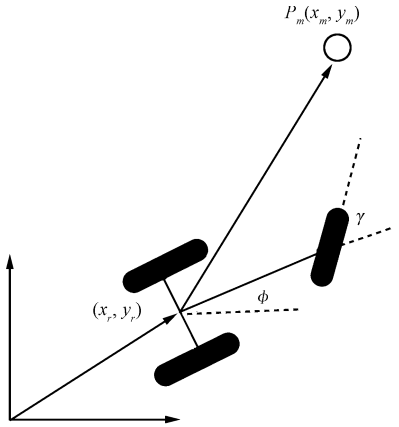

Fig. 1 The robot model

Landmarks are assumed to be stationary, so the process model of landmarks is represented by

$$\boldsymbol{X}_i(k+1) = \boldsymbol{X}_i(k),\ i = 1, 2, \cdots, N \tag{4}$$

So the full system process model of SLAM can be represented by

$$\boldsymbol{X}(k+1) = \boldsymbol{F}(\boldsymbol{X}(k), \nu(k), \gamma(k), \delta\nu, \delta\gamma) \tag{5}$$

$$\boldsymbol{F}(\boldsymbol{X}(k), \nu(k), \gamma(k), \delta\nu, \delta\gamma) = \begin{bmatrix} \phi(k) + \dfrac{(\nu(k)+\delta\nu)T\sin(\gamma(k)+\delta\gamma)}{L} \\ x_r(k) + (\nu(k)+\delta\nu)T\cos(\phi(k)) \\ y_r(k) + (\nu(k)+\delta\nu)T\cos(\phi(k)) \\ \boldsymbol{X}_1(k) \\ \boldsymbol{X}_2(k) \\ \vdots \\ \boldsymbol{X}_N(k) \end{bmatrix} \tag{6}$$

For a range-bearing measurement from the robot to a landmark $\boldsymbol{m}_i = \begin{bmatrix} x_i & y_i \end{bmatrix}^{\mathrm{T}}$, the observation model is represented by range r_i and bearing θ_i as follows:

$$\boldsymbol{Z}_i(k) = \boldsymbol{H}_i(\boldsymbol{X}(k)) + \boldsymbol{\omega}(k) \tag{7}$$

$$\boldsymbol{H}_i(\boldsymbol{X}(k)) = \begin{bmatrix} \sqrt{(x_i(k) - x_r(k)) + (y_i(k) - y_r(k))} \\ \arctan\left(\dfrac{y_i(k) - y_r(k)}{x_i(k) - x_r(k)}\right) \end{bmatrix} \tag{8}$$

where $\boldsymbol{\omega}_i(k) = [\omega_{\nu_i}\ \omega_{\gamma_i}]^{\mathrm{T}}$ is assumed to be Gaussian white noise with zero-mean and the covariance $R_i(k)$.

1.2 EKF SLAM process

1.2.1 Prediction

State prediction:

$$\boldsymbol{X}(k+1|k) = \boldsymbol{F}(\hat{\boldsymbol{X}}(k), \nu(k), \gamma(k), 0, 0) \tag{9}$$

Covariance prediction:

$$P(k+1|k) = \nabla F_{X(k)} P(k|k) \nabla F_{X(k)}^{\mathrm{T}} + \nabla F_{\nu\gamma} Q(k) F_{\nu\gamma}^{\mathrm{T}} \tag{10}$$

where $Q(k)$ is the covariance of control noises $\delta\nu$ and $\delta\gamma$. $\nabla F_{X(k)}$ and $\nabla F_{\nu\gamma}$ are given as follows:

$$\nabla F_{X(k)} = \begin{bmatrix} \nabla F_{\phi X_r(k)} & 0 \\ 0 & I \end{bmatrix},\ \nabla F_{\nu\gamma} = \begin{bmatrix} \nabla f_{\nu\gamma} \\ 0 \end{bmatrix} \tag{11}$$

1.2.2 Update

The estimate state vector can be updated as follows:

$$S(k+1) = \nabla H_i P(k+1|k) \nabla H_i^{\mathrm{T}} + R_{r_i\theta_i} \tag{12}$$

$$\boldsymbol{\mu}(k+1) = \boldsymbol{Z}_i(k+1) - \boldsymbol{H}_i(\hat{\boldsymbol{X}}(k+1|k)) \tag{13}$$

$$W(k+1) = P(k+1|k) \nabla H_i^{\mathrm{T}} S^{-1}(k+1) \tag{14}$$

$$\hat{\boldsymbol{X}}(k+1|k+1) = \hat{\boldsymbol{X}}(k+1|k) + W(k+1)\boldsymbol{\mu}(k+1) \tag{15}$$

The state covariance matrix can be updated by

$$K(k) = P(k+1|k) \nabla H_i^{\mathrm{T}} (\nabla H_i P(k+1|k) \nabla H_i^{\mathrm{T}} + R_i(k))^{-1} \tag{16}$$

$$P(k+1|k+1) = (I - K(k) \nabla H_i) P(k+1|k) \tag{17}$$

If we use information matrix to update covariance, it can be done as follows:

$$\Omega(k+1|k) = P(k+1|k)^{-1} \tag{18}$$

$$\Omega(k+1|k+1) = \Omega(k+1|k) + \nabla H_i^{\mathrm{T}} P(k+1|k)^{-1} \nabla H_i \tag{19}$$

$$\Omega(k+1|k+1) = P(k+1|k+1)^{-1} \tag{20}$$

The Jacobin matrix of measurement function ∇H_i is represented by

$$\nabla H_i = \begin{bmatrix} 0 & -\dfrac{\mathrm{d}x}{\mathrm{d}y} & -\dfrac{\mathrm{d}y}{r} & 0 & \cdots & \dfrac{\mathrm{d}x}{r} & \dfrac{\mathrm{d}y}{r} & 0 & \cdots \\ -1 & \dfrac{\mathrm{d}y}{r^2} & -\dfrac{\mathrm{d}x}{r^2} & 0 & \cdots & -\dfrac{\mathrm{d}y}{r^2} & \dfrac{\mathrm{d}x}{r^2} & 0 & \cdots \end{bmatrix} \tag{21}$$

where $\mathrm{d}x = x_i - x_r(k+1)$, $\mathrm{d}y = y_i - y_r(k+1)$, and $r = \sqrt{(\mathrm{d}x)^2 + (\mathrm{d}y)^2}$.

1.2.3 Augmentation

If the robot observes a landmark which is a new one, it needs to add the landmark as a new state into the system state vectors. When the robot observes the new landmark, the augmentation process can be done as follows:

$$\hat{\boldsymbol{X}}_{\mathrm{aug}}(k) = \begin{bmatrix} \hat{\boldsymbol{X}}(k|k) \\ g_i(\hat{\phi}(k|k),\ \hat{\boldsymbol{X}}_r(k|k),\ \boldsymbol{Z}_i(k)) \end{bmatrix} \tag{22}$$

$$P_{\mathrm{aug}}(k|k) = \begin{bmatrix} P(k|k) & P(k|k)\nabla g_{iX}^{\mathrm{T}} \\ \nabla g_{iX} P(k|k) & \nabla g_{iX}^{\mathrm{T}} P(k|k) \nabla g_{iX} + \nabla g_{iZ}^{\mathrm{T}} R_i(k) \nabla g_{iZ} \end{bmatrix} \tag{23}$$

where $\boldsymbol{g}_i(\hat{\phi}(k|k),\ \hat{\boldsymbol{X}}_r(k|k),\ \boldsymbol{Z}_i(k))$ is represented as

$$\boldsymbol{g}_i(\hat{\phi}(k|k),\ \hat{\boldsymbol{X}}_r(k|k),\ \boldsymbol{Z}_i(k)) = \begin{bmatrix} \hat{x}_r(k|k) + r_i\cos(\hat{\phi}(k|k) + \gamma_i(k)) \\ \hat{y}_r(k|k) + r_i\sin(\hat{\phi}(k|k) + \gamma_i(k)) \end{bmatrix} \tag{24}$$

∇g_{iX} and ∇g_{iZ} are Jacobin matrices of $\boldsymbol{g}_i(\hat{\phi}(k|k),\ \hat{\boldsymbol{X}}_r(k|k),\ \boldsymbol{Z}_i(k))$.

2 Preparations

2.1 Symptoms of inconsistency

The inconsistency manifests in two related symptoms. The first symptom is odd update characteristics of the state mean, resulting in jumps in the vehicle path and linearly constrained localization of the landmark estimates. The second one is wrong information gain (i.e., reduction in uncertainty), such that the estimated covariance is less than the true covariance. In this paper, we focus on the second symptom to analyze the inconsistency. In general, if we can get the true state covariance and the estimated covariance, we can compare the difference between them. Given the true state covariance $P(k)$ and estimated one $P(k|k)$, it is possible to check whether the difference is positive semi-definite. If $P(k|k) - P(k) > 0$, then we say it is consistent, otherwise it is inconsistent.

However, in general, it is difficult to know exactly the true state and true covariance, so we need to design some particular scenarios of EKF SLAM, in which we can easily know the true state and true covariance.

2.2 Particular scenario description

The considered scenario is the same as that of Julier and Uhlmann[15], where the robot keeps stationary and observes just one landmark n times. In that scenario, we assume the position of the landmark is $\begin{bmatrix} x_m & y_m \end{bmatrix}^{\mathrm{T}}$, the robot pose is $\begin{bmatrix} \phi & x & y \end{bmatrix}^{\mathrm{T}}$. When it is the first time to observe the landmark, we need to append the landmark to the state following (22) and (23). The Jacobin matrices in this scenario represented by ∇g_{iX} and ∇g_{iZ} then become

$$\nabla g_{0X} = \begin{bmatrix} -r\sin(\phi + r) & 1 & 0 \\ r\cos(\phi + r) & 0 & 1 \end{bmatrix} \tag{25}$$

$$\nabla g_{0Z} = \begin{bmatrix} \cos(\phi + r) & -r\sin(\phi + r) \\ \sin(\phi + r) & r\cos(\phi + r) \end{bmatrix} \tag{26}$$

Denote the inverse of ∇g_{0Z} as G. We can easily get G as

$$G = \frac{1}{r^2} \begin{bmatrix} r\cos(\phi + r) & r\sin(\phi + r) \\ -\sin(\phi + r) & \cos(\phi + r) \end{bmatrix} \tag{27}$$

Denote a useful matrix T as $T = G\nabla g_{0X}$ and another matrix B as

$$B = \begin{bmatrix} T^{\mathrm{T}} \\ G^{\mathrm{T}} \end{bmatrix} \tag{28}$$

The Jacobin matrices defined by (21) is

$$\nabla H = \begin{bmatrix} 0 & -\dfrac{\mathrm{d}x}{\mathrm{d}y} & -\dfrac{\mathrm{d}y}{r} & \dfrac{\mathrm{d}x}{r} & \dfrac{\mathrm{d}y}{r} \\ -1 & \dfrac{\mathrm{d}y}{r^2} & -\dfrac{\mathrm{d}x}{r^2} & -\dfrac{\mathrm{d}y}{r^2} & \dfrac{\mathrm{d}x}{r^2} \end{bmatrix} \tag{29}$$

Denote some temporal matrices as follows:

$$A = \begin{bmatrix} \dfrac{\mathrm{d}x}{r} & \dfrac{\mathrm{d}y}{r} \\ -\dfrac{\mathrm{d}y}{r^2} & \dfrac{\mathrm{d}x}{r^2} \end{bmatrix}, \quad \boldsymbol{e} = \begin{bmatrix} 0 \\ 1 \end{bmatrix} \tag{30}$$

$$A_e = \begin{bmatrix} A^{-1}\boldsymbol{e} & I \end{bmatrix} \tag{31}$$

where $\mathrm{d}x = x_m - x, \mathrm{d}y = y_m - y$, and $r = \sqrt{\mathrm{d}x^2 + \mathrm{d}y^2}$.

2.3 Theorems to analyze inconsistency

Theorem 1. If the robot is stationary at a point and observes a landmark n times, at the same time the Jacobin matrices are evaluated in the true state, and the landmarks are initialized by (22) and (23), then the covariance matrix of robot pose and the covariance matrix of landmark satisfy the following equation

$$P = P_{\mathrm{temp}} - P_{\mathrm{temp}}B(R + B^{\mathrm{T}}P_{\mathrm{temp}}B)^{-1}B^{\mathrm{T}}P_{\mathrm{temp}} \tag{32}$$

where B is denoted as (28). R is the covariance of the measurement noise and P_{temp} is the same as P^n_{end} denoted in [3] as follows:

$$P_{\mathrm{temp}} = \begin{bmatrix} P_0 & P_0A_e^{\mathrm{T}} \\ A_eP_0 & A_eP_0A_e^{\mathrm{T}} + \dfrac{A^{-1}RA^{-\mathrm{T}}}{n-1} \end{bmatrix} \tag{33}$$

where P_0 is the initial robot pose uncertainty, A_e as denoted in (31) and A as represented in (30).

Proof. If the initial uncertainty of the robot is P_0, the initial position states are $\begin{bmatrix} \phi & x & y \end{bmatrix}^{\mathrm{T}}$ and the covariance of the measurement noise is R, then when the robot observes the landmark for the first time, we need to use (22) and (23) to do initialization and append the landmark to system states. The new covariance is as follows:

$$P_1 = \begin{bmatrix} P_0 & P_0\nabla g_{0X}^{\mathrm{T}} \\ \nabla g_{0X}P_0 & \nabla g_{0X}^{\mathrm{T}}P_0\nabla g_{0X} + \nabla g_{0Z}^{\mathrm{T}}R\nabla g_{0Z} \end{bmatrix} \tag{34}$$

where ∇g_{0X} and ∇g_{0Z} are denoted in (25) and (26), respectively. By using matrix inverse lemma in Appendix A, we get

$$\Omega_1 = P_1^{-1} = \begin{bmatrix} P_0^{-1} + T^{\mathrm{T}}R^{-1}T & T^{\mathrm{T}}R^{-1}G \\ G^{\mathrm{T}}R^{-1}T & G^{\mathrm{T}}R^{-1}G \end{bmatrix} \tag{35}$$

where T is denoted as above and G is denoted as (27). When the robot sees the landmark the second time to n-th time, we use (10) to predict and use (18) $\sim$ (20) to do covariance update iteratively. For the robot is stationary, we can get

$$P(k+1|k) = P(k|k) \tag{36}$$

By using (18) $\sim$ (20) and (36) n times, we can get

$$\begin{aligned} \Omega_n &= \Omega_1 + (n-1)\nabla H^{\mathrm{T}}R^{-1}\nabla H = \\ &\quad \begin{bmatrix} P_0^{-1} + T^{\mathrm{T}}R^{-1}T & T^{\mathrm{T}}R^{-1}G \\ G^{\mathrm{T}}R^{-1}T & G^{\mathrm{T}}R^{-1}G \end{bmatrix} + \\ &\quad (n-1)\begin{bmatrix} -H^{\mathrm{T}} \\ A^{\mathrm{T}} \end{bmatrix} R^{-1}\begin{bmatrix} -H & A \end{bmatrix} = \\ &\quad \begin{bmatrix} T^{\mathrm{T}}R^{-1}T & T^{\mathrm{T}}R^{-1}G \\ G^{\mathrm{T}}R^{-1}T & G^{\mathrm{T}}R^{-1}G \end{bmatrix} + \\ &\quad \begin{bmatrix} P_0^{-1} + (n-1)H^{\mathrm{T}}R^{-1}H & -(n-1)H^{\mathrm{T}}R^{-1}A \\ -(n-1)A^{\mathrm{T}}R^{-1}H & (n-1)A^{\mathrm{T}}R^{-1}A \end{bmatrix} = \\ &\quad BR^{-1}B^{\mathrm{T}} + \Omega_{\mathrm{temp}} \end{aligned} \tag{37}$$

where Ω_{temp} is the inverse of P_{temp}. By using the matrix inverse lemma in Appendix A, we get

$$\begin{aligned} &P = \Omega^{-1} = \\ &(BR^{-1}B^{\mathrm{T}} + \Omega_{\mathrm{temp}})^{-1} = \\ &P_{\mathrm{temp}} - P_{\mathrm{temp}}B(R + B^{\mathrm{T}}P_{\mathrm{temp}}B)^{-1}B^{\mathrm{T}}P_{\mathrm{temp}} \end{aligned} \tag{38}$$

□

Theorem 1 gives the equation that the estimated covariance matrix must obey. It is shown that the covariance matrix is different with the result in [14]. This is because that we have done landmark initialization and augmentation and considered the effect of measurement noise in the first step.

Theorem 2. Assume $R_\alpha = \alpha I_2$ $(0 < \alpha < +\infty)$ in (32). If $0 < \alpha_1 < \alpha_2 < +\infty$, then $P(\alpha_2) > P(\alpha_1) > 0$, where $P(\alpha) = P_{\text{temp}}(\alpha) - P_{\text{temp}}(\alpha)B(R_\alpha + B^{\text{T}}P_{\text{temp}}(\alpha)B)^{-1}B^{\text{T}}P_{\text{temp}}(\alpha)$.

Proof. By (38), we easily get $P(\alpha) > 0$ and $P^{-1}(\alpha) = BR_\alpha^{-1}B^{\text{T}} + \Omega_{\text{temp}}(\alpha)$, where $\Omega_{\text{temp}}(\alpha) = P^{-1}(\alpha)$ is represented by

$$\Omega_{\text{temp}}(\alpha) = \begin{bmatrix} P_0^{-1} + T^{\text{T}}R_\alpha^{-1}T & T^{\text{T}}R_\alpha^{-1}G \\ G^{\text{T}}R_\alpha^{-1}T & G^{\text{T}}R_\alpha^{-1}G \end{bmatrix} \tag{39}$$

Computing the difference between $P^{-1}(\alpha_1)$ and $P^{-1}(\alpha_2)$, and we get

$$P^{-1}(\alpha_1) - P^{-1}(\alpha_2) = \left(\frac{1}{\alpha_1} - \frac{1}{\alpha_2}\right)\left[BB^{\text{T}} + (n-1)\nabla H^{\text{T}}\nabla H\right] > 0 \tag{40}$$

Because of $0 < \alpha_1 < \alpha_2 < +\infty$, by Appendix B, we easily get $P(\alpha_2) > P(\alpha_1) > 0$. □

Theorem 2 means that the estimated state covariance matrix decreases monotonically as the measurement noise covariance decreases monotonically. This indicates that the measurement noise covariance matrix can increase the accuracy of the full covariance, and it contains rich update information, however it may also contain too much information, which results in EKF SLAM inconsistency. The results can be seen in Fig. 2.

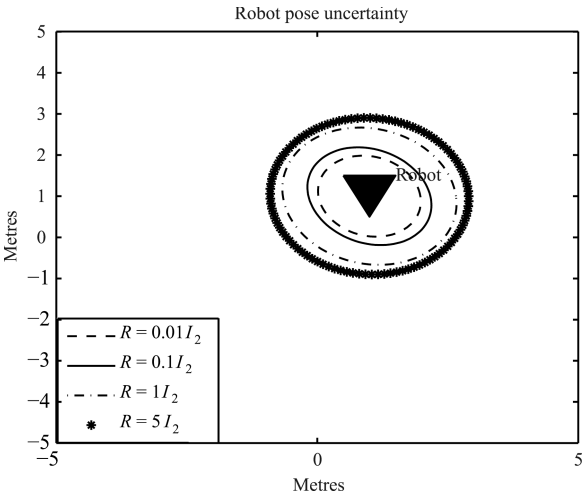

Fig. 2 Different robot poses uncertainty when given different measurement noise (Seeing Theorem 2, the initial robot pose uncertainty is $P_0 = \text{diag}\{0.5, 2, 2\}$. All the Jacobin matrices are evaluated in the true state, and the observation time is fixed as 200.)

Theorem 3. If $R_\alpha = \alpha I_2$ $(0 < \alpha < +\infty)$ in (32), then $0 < P_{k+1}(\alpha) < P_k(\alpha)$, where $P_k(\alpha) = P_{\text{temp}}^k - P_{\text{temp}}^k B(R + B^{\text{T}}P_{\text{temp}}^k B)^{-1}B^{\text{T}}P_{\text{temp}}^k$, $P_{\text{temp}}^k = P_{\text{temp}} \mid n = k\,(k = 1, 2, \cdots, n-1)$.

Proof. Computing the difference between $P_{k+1}^{-1}(\alpha)$ and $P_k^{-1}(\alpha)$, we get

$$P_{k+1}^{-1}(\alpha) - P_k^{-1}(\alpha) = \frac{1}{\alpha}\nabla H^{\text{T}}H > 0 \tag{41}$$

Because $P_k(\alpha) > 0$ $(k = 1, 2, 3, \cdots, n-1)$, by Appendix B, we get $0 < P_{k+1}(\alpha) < P_k(\alpha)$. □

Theorem 3 shows that as the measurement time increases, the full-estimated covariance matrix decreases monotonically. This means that by increasing the observation times, it can increase useful information to reduce the uncertainty of the full system states. However, it also may contain redundant information to update the full system, which results in inconsistency. The results can be seen in Fig. 3.

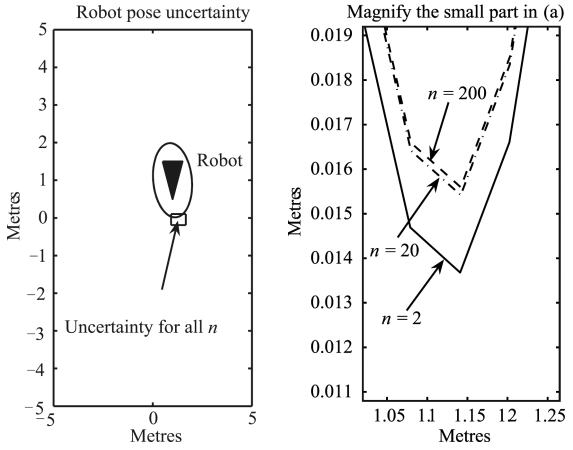

(a) Robot poses uncertainty with different n

(b) Magnifying version of small part in (a) (Seeing Theorem 3, the initial robot pose uncertainty is $P_0 = \text{diag}\{0.5, 2, 2\}$. All the Jacobin matrices are evaluated in the true state and the measurement noise covariance is $R = \text{diag}\{0.01, 0.01\}$.)

Fig. 3 Different robot poses uncertainties by different observation times when given measurement noise

Corollary 1. Assume that the robot is stationary at a point and observes a landmark for n times. If it uses basic EKF SLAM algorithm with (22) and (23) to do initialization and augmentation, and uses the same true state to compute Jacobin matrices, when $n \to +\infty$, then the full-state covariance matrix can reach the lower bound as follows:

$$P_\infty = P_{\text{temp}}^\infty - P_{\text{temp}}^\infty B(R + B^{\text{T}}P_{\text{temp}}^\infty B)^{-1}B^{\text{T}}P_{\text{temp}}^\infty \tag{42}$$

where

$$P_{\text{temp}}^\infty = \begin{bmatrix} P_0 & P_0A_e^{\text{T}} \\ A_eP_0 & A_eP_0A_e^{\text{T}} \end{bmatrix} \tag{43}$$

Proof. By Theorem 3, when $n \to +\infty$, (42) can be easily derived from (32) and (33). □

This corollary shows the lower bound of the full-state covariance matrix, when given the measurement noise. It is useful to analyze the effect of observation times on consistency, and it implies that the effect of observation time on the degree of inconsistency has an upper bound. The result can be seen in Fig. 4.

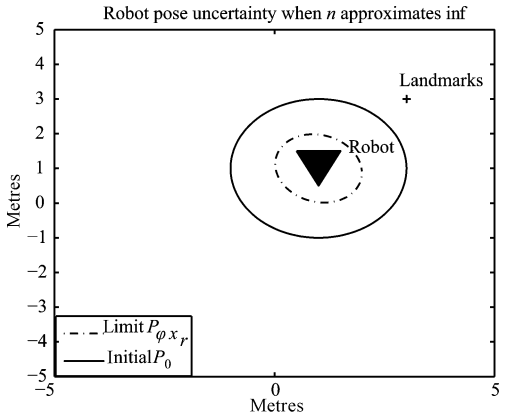

Fig. 4 The lower bound of robot pose uncertainty when observation times $n \to +\infty$ (Seeing Corollary 1, the initial robot uncertainty is $P_0 = \mathrm{diag}\{0.5, 2, 2\}$. The measurement noise is $R = \mathrm{diag}\{0.01, 0.01\}$ and all the Jacobin matrices are evaluated in true state.)

Corollary 2. If $R_\alpha = \alpha I_2$ $(0 < \alpha < +\infty)$ in (32), when $\alpha \to +\infty$, $\lim_{n\to+\infty} \frac{\alpha}{n} = 0$, then the full-state estimated covariance matrix becomes a fixed one as

$$P_\infty(\infty) = \begin{bmatrix} P_0 & P_0 A_e^{\mathrm{T}} \\ A_e P_0 & A_e P_0 A_e^{\mathrm{T}} \end{bmatrix} \tag{44}$$

Proof. By Theorem 1, when $\alpha \to +\infty$, $\lim_{n\to+\infty} \frac{\alpha}{n} = 0$, (44) can be easily derived from (32) and (33). □

Corollary 2 gives a useful result, which can be used to investigate the integrated effect of observation time and measurement noise on the inconsistency.

3 Consistency analysis

Based on these theorems above, we give an important theorem to investigate the inconsistency caused by measurement noise and observation time. Then, we use simulations to analyze the results.

3.1 Theoretical analysis on inconsistency

Theorem 4. Assume that the robot is stationary at a point and only observes a landmark for n times. If it uses basic EKF SLAM algorithm with (22) and (23) to do initialization and augmentation and uses the same true state to compute Jacobin matrices, then the EKF SLAM inconsistency is mainly affected by the measurement noise covariance matrix and observation time. The degree of the inconsistency is also determined by R and observation time n.

Proof. After n steps, we can compute the ultimate estimated information matrix as follows:

$$\begin{aligned} \Omega_n &= \Omega_1 + \sum_{j=2}^{n} \nabla \tilde{H}_j^{\mathrm{T}} R^{-1} \nabla \tilde{H}_j = \\ &\quad \begin{bmatrix} P_0^{-1} + T^{\mathrm{T}} R_\alpha^{-1} T & T^{\mathrm{T}} R_\alpha^{-1} G \\ G^{\mathrm{T}} R_\alpha^{-1} T & G^{\mathrm{T}} R_\alpha^{-1} G \end{bmatrix} + \\ &\quad \sum_{j=2}^{n} \begin{bmatrix} -\tilde{H}_j^{\mathrm{T}} \\ \tilde{A}_j^{\mathrm{T}} \end{bmatrix} R^{-1} \begin{bmatrix} -\tilde{H}_j & \tilde{A}_j \end{bmatrix} \end{aligned} \tag{45}$$

where $\nabla \tilde{H}_j$ is the Jacobin matrix computed in predicted state, and $\tilde{H}_j$ and $\tilde{A}_j$ are the same parts in $\nabla \tilde{H}_j$ computed by predicted state.

By assumption that all the Jacobins are computed in true state values, so $\tilde{H}_j = H$, $\tilde{A}_j = A$ $(j = 2, 3, \cdots, n)$, then (45) becomes (37). By Theorem 1, we can get the ultimate results of estimated covariance matrix as

$$P = P_{\mathrm{temp}} - P_{\mathrm{temp}} B (R + B^{\mathrm{T}} P_{\mathrm{temp}} B)^{-1} B^{\mathrm{T}} P_{\mathrm{temp}} \tag{46}$$

In (46), $R_\alpha = \alpha I$ $(0 < \alpha < +\infty)$. When $\alpha \to +\infty$, we get

$$P_n(\infty) = \begin{bmatrix} P_0 & P_0 \nabla g_{0X}^{\mathrm{T}} \\ \nabla g_{0X} P_0 & +\infty \end{bmatrix} \tag{47}$$

By Corollary 2, when $0 < \alpha < +\infty$, $n < +\infty$, we can get

$$P_n(\alpha) < P_n(\infty) = \begin{bmatrix} P_0 & P_0 \nabla g_{0X}^{\mathrm{T}} \\ \nabla g_{0X} P_0 & +\infty \end{bmatrix} \tag{48}$$

By the property in (3) in Appendix B, we can get

$$P_{n\phi X_r}(\alpha) < P_0 \tag{49}$$

where $P_{n\phi X_r}(\alpha)$ is the estimated covariance of the robot pose.

This means that the uncertainty of the robot pose is decreased. However, it is known that when the robot is stationary and only observes one landmark, in which it can not change the uncertainty of the robot pose[14−15]. So this is incorrect (inconsistent). Furthermore, by Theorem 2, when observation time is fixed, it is shown that the larger the measurement noise, the larger the estimated covariance matrix. This means increase in the measurement noise can reduce the inconsistency. So, when observation time is fixed, the degree of the inconsistency is determined by measurement noise R. When $R \to +\infty$, it almost has no effect on inconsistency. In the other aspect, if given $R_\alpha = \alpha I$ $(0 < \alpha < +\infty)$, then when $1 < k < n$, by Theorem 3, we get

$$P_k(\alpha) < P_1(\alpha) = \begin{bmatrix} P_0 & P_0 \nabla g_{0X}^{\mathrm{T}} \\ \nabla g_{0X} P_0 & \nabla g_{0X}^{\mathrm{T}} P_0 \nabla g_{0X} + \nabla g_{0Z}^{\mathrm{T}} R \nabla g_{0Z} \end{bmatrix} \tag{50}$$

By the property in (3) in Appendix B, we can get

$$P_{k\phi X_r}(\alpha) < P_0 \tag{51}$$

This means that given a measurement noise, as the observation time increases, the uncertainty of the robot pose is decreased. While this is contradicted with the fact that the robot is stationary and the pose can not be changed. So this is wrong (inconsistent). It can be seen that when observation time increases, the inconsistency is inevitable. Furthermore, by Theorem 3 and given measurement noise, the more the observation time, the less the estimated state covariance. This means that increase in observation time increases the inconsistency. So, when measurement noise is fixed, the degree of inconsistency is determined by observation time. □

Theorem 4 demonstrates the two kinds of important information in our considering situation. The first one is that the observation time and measurement noise can cause the EKF SLAM to be inconsistent. The second one is that it shows the individual effect of measurement noise or observation time to inconsistency given the other.

In fact, by Corollaries 1 and 2 and Theorem 4, we can further investigate the integrated effect of the two factors on the inconsistency. By Corollary 1, we know that given measurement noise, when the observation time $n \to \infty$, the estimated state covariance matrix will approximate the lower bound by (42), and it will become the most inconsistent. However, by Corollary 2, when $\alpha \to +\infty$, $\lim_{n\to+\infty} \frac{\alpha}{n} = 0$,

the estimated robot pose covariance matrix becomes the initial one, and the algorithm will become consistent. By Theorem 4, it is implied that increasing the measurement noise can reduce the inconsistency of the algorithm and at the same time can reduce the inconsistency caused by observation time. In other words, the degree of increasing the consistency by magnifying the measurement noise is greater than the degree of decreasing the consistency by increasing the observation time.

3.2 Simulation analysis

We assume the robot is stationary and only observes a landmark. To focus on the effects of measurement noise and observation time on inconsistency, we compute all the Jacobin matrices in the true states. Fig. 5 shows the individual effect of observation time on inconsistency. In Fig. 5, we assumed the robot was at $(1, 1)$, the landmark was located at $(3, 3)$ and the measurement noise was fixed as $R = \text{diag}\{0.01, 0.01\}$. We used the algorithm to run 2, 20, and 200 times. It was showm that with the observation times increasing, the algorithm became inconsistent. The more observation time, the more inconsistency, but the velocity of decreasing consistency was slow when the observation time became large. Fig. 6 shows the independent effect of measurement noise on inconsistency. The initial value was the same as Fig. 5. The difference was that we fixed observation time as 200 while varying the measurement covariance matrices. Fig. 6 shows that given the observation time, increasing the measurement noise can increase the algorithm consistency. Fig. 7 shows the results of the integrated effects of measurement noise and observation time on inconsistency. In that simulation, except the landmark localization was $(5, 5)$, the others were the same as Fig. 6. In Fig. 7, we can see that increasing the observation time very greatly while increasing the covariance matrix of the measurement noise a little can still decrease the inconsistency. This means that the rate of decreasing the inconsistency by increasing the measurement noise is much greater than that of increasing the inconsistency by increasing observation time. So, magnifying the measurement noise can compensate for the inconsistency caused by increasing observation time.

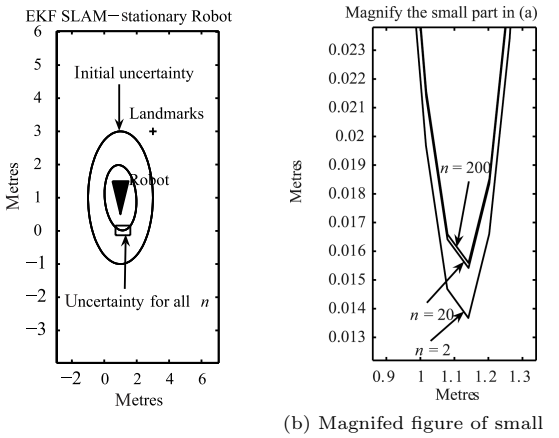

(a) Robot poses uncertainty with different n

(b) Magnifed figure of small part in (a) (Seeing Theorem 4, all the Jacobin matrices are evaluated in the true state.)

Fig. 5 The effect of observation time on inconsistency

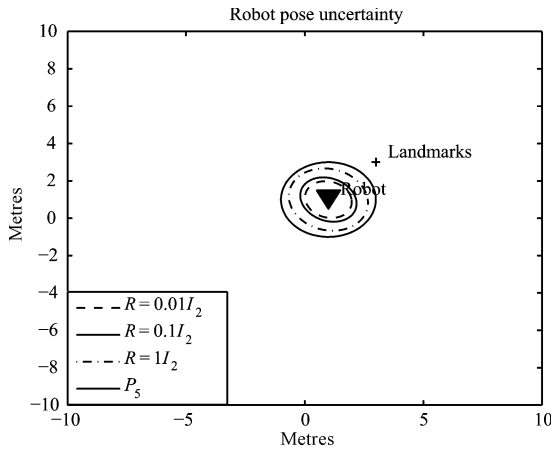

Fig. 6 The effect of measurement noise on inconsistency (Seeing Theorem 4, all the Jacobin matrices were evaluated in the true state.)

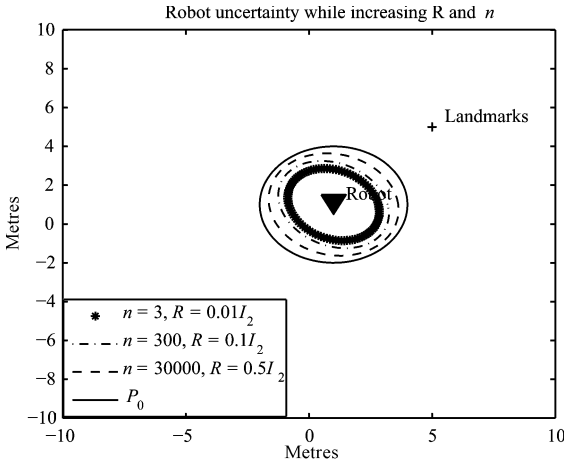

Fig. 7 The integrated effect of measurement noise and observation time on inconsistency (All the Jacobin matrices were evaluated in true state.)

4 Discussion

Consistency issue is a fundamental problem in SLAM. It has been shown recently that EKF SLAM can produce inconsistent (overconfident) estimations by a number of researchers. The theoretical results in this paper not only confirm those claims but also give new insights in understanding the problem. Previous investigations of EKF-SLAM consistency[13, 15, 18−20] claimed that the algorithm′s failure is time dependent, but they only gave some simulation results. Our results agree with them, at the same time, we give an explicit theoretical explanation to them. We show that with the observation time increasing, the inconsistency is inevitable. Most recently, Bailey[16] uses Monte Carlo simulation to analyze the inconsistency problem, and gave two symptoms of inconsistency and derived the some special results. Huang[14] gave some theoretical explanations to inconsistency caused by linearization errors and large heading orientation and they well explained the results in [11, 13, 15, 19−20]. However, they ignored the landmark appending process and did not consider the effect of process noise and measurement noise. Moreover, no earlier work pointed out whether the measurement noise can cause the inconsistency or how it affects the inconsistency.

In this paper, we analyzed the effect of measurement noise on inconsistency in theory. Our results are that the measurement noise is also a factor to cause inconsistency and the larger the covariance matrix of measurement noise, the less effect on inconsistency.

In Theorem 4, we assumed the Jacobin matrix is computed at the true state values, and we got some useful results of inconsistency caused by observation time and measurement noise. In fact, if we assume $R \to \infty$, then (45) reduces to (66) in [14]. So we could derive the same results as [14] to analyze the effects of heading orientation and Jacobin matrices evaluated in different states on inconsistency. This means that without considering the effect of measurement noise and ignoring the effects of observation times, our analysis could also get the same results as in [14, 16].

The common ideas this paper based on to analyze the inconsistency is "keep observing new landmarks does not help in reducing the robot pose uncertainty", which is also the basic idea used in [14−16]. In this paper, we give the theoretical results of inconsistency caused by the observation time and measurement noise. One should pay attentions to the assumptions: 1) All the results are based on that the robot is stationary; 2) The map is points and the measurements are range and bearing which is ideal; 3) The landmark initialization and state augmentation are based on (22) and (23); and 4) The data association is assumed to be known.

Although this paper only analyzes the situation that the robot is stationary, in fact, it is a particular situation of movement without considering the effects of process noise and nonlinearity of robot model on consistency. So the theoretical results in this paper are also useful in moving situation in some aspects: 1) The measurement noise and observation time are also the factors to cause inconsistency in robot moving situation; 2) When the other parameters have enough small effects on inconsistency, the theoretical results in this paper are almost true to moving situation; 3) The results in this paper may provide possible foundation to analyze the independent effects of process noise and nonlinearity of robot model, and even effects of all parameters on inconsistency in robot moving situation. However, to investigate the inconsistency in moving situation, besides measurement noise and observation time, effects of process noise and nonlinearity of robot model on consistency should be considered. Moreover, the possible coupling of the four factors should also be analyzed.

Inconsistency analysis can give some insights to use EKF SLAM in practice. Through our theoretical investigations, it is shown that when the observation time becomes great, the inconsistency is inevitable. So to get robust and consistent SLAM algorithms, we can choose some EKF SLAM variants to minimize the inconsistency. Furthermore, it is also shown that increasing the measurement noise can cause less inconsistency. The rate of improvement to consistency by increasing the measurement noise is greater than that of the damaging the consistency by increasing the observation time. So in some situations, we can magnify the measurement noise to compensate for inconsistency by observation time and to reduce the inconsistency.

5 Conclusions

In this paper, we investigated the effects of measurement noise and observation time on inconsistency of EKF SLAM in theory. The algorithm uses points as landmarks and observations with range-bearings. Using simple and basic scenario and general augmentation method, we deduced some theorems on inconsistency of the full-estimated state covariance matrix. Through analysis, we got the results of effects of measurement noise and observation time on inconsistency. We showed that the observation time and measurement noise are factors to cause inconsistency in our situation. Moreover, with the observation time increasing, the inconsistency will increase and it will become inevitable, but it will have an upper bound. At the same time, increasing the measurement noise can slow the accumulation of inconsistency and prolong the SLAM time. Investigating the effects of measurement noise, process noise, and observation time on inconsistency when the robot moves in the environment needs further work.

Appendix A

Matrix inversion lemma

Lemma A1. Suppose the partitioned matrix

$$M = \begin{bmatrix} A & B \\ C & D \end{bmatrix} \tag{A1}$$

where A and D are square matrices. Then the inversion of M can be evaluated by

$$M^{-1} = \begin{bmatrix} X & Y \\ U & V \end{bmatrix} \tag{A2}$$

Here, if A is invertible, then

$$\begin{aligned} X &= A^{-1} - A^{-1}B(D - CA^{-1}B)^{-1}CA^{-1} \\ Y &= -A^{-1}B(D - CA^{-1}B)^{-1} \\ U &= -(D - CA^{-1}B)^{-1}CA^{-1} \\ V &= (D - CA^{-1}B)^{-1} \end{aligned} \tag{A3}$$

If D is invertible, then

$$\begin{aligned} X &= (A - BD^{-1}C)^{-1} \\ Y &= -(A - BD^{-1}C)^{-1}BD^{-1} \\ U &= -D^{-1}C(A - BD^{-1}C)^{-1} \\ V &= D^{-1} - D^{-1}C(A - BD^{-1}C)^{-1}BD^{-1} \end{aligned} \tag{A4}$$

Thus, if both A and D are invertible, then

$$(A - BD^{-1}C)^{-1} = A^{-1} + A^{-1}B(D - CA^{-1}B)^{-1}CA^{-1} \tag{A5}$$

when $B = C^{\mathrm{T}}$, then

$$(A + BD^{-1}C)^{-1} = A^{-1} + A^{-1}B(D + CA^{-1}B)^{-1}CA^{-1} \tag{A6}$$

Appendix B

Property of positive semi-definite matrices (psd)

1) If $A \in \mathbf{R}^{n\times n}$ is psd, then for any matrix $B \in \mathbf{R}^{n\times n}$, BAB^{T} is psd.

2) Given $A \in \mathbf{R}^{n\times n}$, $A > 0$, $B \in \mathbf{R}^{n\times n}$, and $B > 0$, if $A > B$, then $A^{-1} < B^{-1}$.

3) Given $A \in \mathbf{R}^{n\times n}$, $A > 0$, $B \in \mathbf{R}^{n\times n}$ and $B > 0$, if $A > B$, $A = \begin{bmatrix} A_{11} & A_{12} \\ A_{21} & A_{22} \end{bmatrix}$, and $B = \begin{bmatrix} B_{11} & B_{12} \\ B_{21} & B_{22} \end{bmatrix}$, then $A_{11} > B_{11}$ and $A_{22} > B_{22}$, where A_{11}, A_{22} and B_{11}, B_{22} are sub-square matrices.

References

1 Smith R, Self M, Cheeseman P. A stochastic map for uncertain spatial relationships. In: Proceedings of International Symposium of Robotics Research. Santa Clara, USA: MIT Press, 1988. 467−474

2 Frese U, Larsson P, Duckett T. A multilevel relaxation algorithm for simultaneous localization and mapping. *IEEE Transactions on Robotics*, 2005, **21**(2): 196−207

3 Estrada C, Neria J, Tardos J D. Hierarchical SLAM: real-time accurate mapping of large environments. *IEEE Transactions on Robotics*, 2005, **21**(4): 588−596

4 Guivant J E, Nebot E M. Optimization of the simultaneous localization and map-building algorithm for real-time implementation. *IEEE Transactions on Robotics and Automation*, 2001, **17**(3): 242−257

5 Thrun S, Liu Y, Koller D, Ng A Y, Ghahramani Z, Durrant-Whyte H. Simultaneous localisation and mapping with sparse extended information filters. *International Journal of Robotics Research*, 2004, **23**(7-8): 693−716

6 Montemerlo M, Thrun S, Koller D, Wegbreit B. Fast-SLAM 2.0: an improved particle filtering algorithm for simultaneous localization and mapping that provably converges. In: Proceedings of International Joint Conference on Artificial Intelligence. Acapulco, Mexico: Lawrence Erlbaum Associates Ltd, 2003. 1151−1156

7 Guivant J, Netbot E. Improving computational and memory requirements of simultaneous localization and map building algorithms. In: Proceedings of IEEE International Conference on Robotics and Automation. Washington D. C., USA: IEEE, 2002. 2731−2736

8 Durrant-Whyte H, Bailey T. Simultaneous localization and mapping: part I. *IEEE Robotics Automation and Magazine*, 2006, **13**(6): 99−107

9 Bailey T, Durrant-Whyte H. Simultaneous localization and mapping: part II. *IEEE Robotics Automation and Magazine*, 2006, **13**(6): 108−117

10 Neira J, Tardos J D. Data association in stochastic mapping using the joint compatibility test. *IEEE Transactions on Robotics and Automation*, 2001, **17**(6): 890−897

11 Davey S J. Simultaneous localization and map building using the probabilistic multi-hypothesis tracker. *IEEE Transactions on Robotics*, 2007, **23**(2): 271−280

12 Bailey T. Mobile Robot Localisation and Mapping in Extensive Outdoor Environments [Ph. D. dissertation], University of Sydney, Australian Center for Field Robotics, Australian, 2002

13 Frese U. A discussion of simultaneous localization and mapping. *Autonomous Robots*, 2006, **20**(1): 25−42

14 Huang S, Dissanayake G. Convergence and consistency analysis for extended Kalman filter based SLAM. *IEEE Transactions on Robotics*, 2007, **23**(5): 1036−1049

15 Julier S J, Uhlmann J K. A counter example to the theory of simultaneous localization and map building. In: Proceedings of IEEE Conference on Robotics and Automation. Seoul, Korea: IEEE, 2001. 4238−4243

16 Bailey T, Nieto J, Guivant J, Stevens M, Nebot E. Consistency of the EKF-SLAM algorithm. In: Proceedings of IEEE/RSJ International Conference on Intelligence Robots and Systems. Beijing, China: IEEE, 2006. 3562−3568

17 Bailey T, Nieto J, Nebot E. Consistency of the fast SLAM algorithm. In: Proceedings of IEEE International Conference on Robotics and Automation. Orlando, USA: IEEE, 2006. 424−429

18 Leonard J J, Newman P M. Consistent, convergent and constant-time SLAM. In: Proceedings of International Joint Conference on Artificial Intelligence. Acapulco, Mexico: IEEE, 2003. 1143−1150

19 Castellanos J A, Neira J, Tardos J D. Limits to the consistency of EKF-based SLAM. In:Proceedings of the 5th IFAC Symposium on Intelligent Autonomous Vehicles. Lisbon, Portugal: ACM, 2004. 1−2

20 Martinell A, Tomatis N, Siegwart R. Some results on SLAM and the closing the loop problem. In: Proceedings of IEEE/RSJ International Conference on Intelligence Robots and Systems. Edmonton, Canada: IEEE, 2005. 2917−2922

21 Castellanos J A, Martinez-Cantin R, Tarods J D, Neira J. Robocentric map joining: improving the consistency of EKF-SLAM. *Robotics and Autonomous Systems*, 2007, **55**(1): 21−29

22 Rodriguez-Losada D, Matia F, Jimenez A, Galan R. Consistency improvement for SLAM-EKF for indoor environments. In: Proceedings of IEEE Conference on Robotics and Automation. Orlando, USA: IEEE, 2006. 418−423

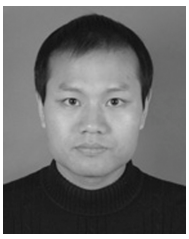

LI Hui-Ping Ph. D. candidate at the College of Marine Engineering, Northwestern Polytechnical University. He received his bachelor degree from Northwestern Polytechnical University in 2006. His research interest covers nonlinear filter, simultaneous localization and mapping, and robot navigation. Corresponding author of this paper. E-mail: 888.li.mmm@163.com

XU De-Min Professor at Northwestern Polytechnical University (NWPU), academician of Chinese Academy of Engineering. He graduated from NWPU in 1961 and completed his postgraduate study in 1964. From 1987 to 1988, he was a visiting scholar in the Department of Electrical Engineering and Computer Science, University of Michigan (U.S.). His main research interest is autonomous underwater vehicle (AUV). E-mail: xudm@nwpu.edu.cn

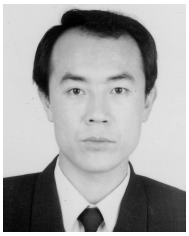

ZHANG Fu-Bin Assistant professor at the College of Marine Engineering, Northwestern Polytechnical University. He received his Ph. D. degree from Northwestern Polytechnical University in 2008. His research interest covers precise guidance, control and navigation of autonomous underwater vehicles.
E-mail: zhangfubin@nwpu.edu.cn

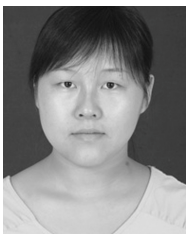

YAO Yao Ph. D. candidate at the College of Marine Engineering, Northwestern Polytechnical University. She received her bachelor degree from Northwestern Polytechnical University in 2005. Her research interest covers precise guidance, control and simulation with particular attention to cooperative localization of multiple vehicles. E-mail: yaoyao@mail.nwpu.edu.cn